Journal of Applied Physics ARTICLE pubs.aip.org/aip/jap

# Impact of swift heavy oxygen ion irradiation on the performance of Pt/GaN Schottky diodes and epitaxial layers: A comparative study

Cite as: J. Appl. Phys. **134**, 165704 (2023); doi: 10.1063/5.0171363
Submitted: 8 August 2023 · Accepted: 10 October 2023 ·
Published Online: 27 October 2023



Kamal Singh,[1] Parmod Kumar,[2] Vaishali Rathi,[1] Tanuj Kumar,[3] Ratnesh K. Pandey,[1] D. Kanjilal,[4] Ranjeet K. Brajpuriya,[1] and Ashish Kumar[1,5,a)]

## AFFILIATIONS

[1]Department of Physics (SoE), University of Petroleum and Energy Studies, Bidholi, Dehradun 248007, India
[2]Department of Physics, J. C. Bose University of Science and Technology, YMCA Faridabad 136119, India
[3]Department of Nano Science and Material, Central University of Jammu, Rahya-Suchani, Samba, Jammu 181143, India
[4]Inter University Accelerator Centre, Aruna Asaf Ali Marg, Vasantkunj, New Delhi 110067, India
[5]Department of Physics and Astronomical Sciences, Central University of Jammu, Rahya-Suchani, Samba, Jammu 181143, India

[a)]**Author to whom correspondence should be addressed:** dr.akmr@gmail.com and ashish.phy@cujammu.ac.in

## ABSTRACT

Pt/GaN Schottky barrier diodes and GaN epitaxial layers on sapphire substrates were studied under swift heavy ion irradiation using 100 MeV $O^{7+}$ ions having fluences in the range of $1 \times 10^{10}$–$6.4 \times 10^{13}$ ions/cm$^2$. It was observed that ideality factor, Schottky barrier height, and series resistance increased, while carrier concentration decreased with increasing ion fluence. The *ex situ* measurements, such as x-ray diffraction and UV–Vis spectroscopy, revealed that GaN layers exhibit negligible variation in structural and bandgap characteristics after irradiation with oxygen ions. The cross-sectional transmission electron microscopy images of the GaN epitaxial layer irradiated at $5 \times 10^{12}$ ions/cm$^2$ confirmed the absence of irradiation-induced tracks or defect clusters, indicating only point defects that can act as charge traps without structural damage.





## INTRODUCTION

The strategic importance of GaN technology has been indicated by its diverse applications in power and optoelectronic devices like HEMTs, LEDs, and lasers. GaN has also found potential applications in emerging technologies of nuclear reactors, satellites, and other avionic industries because of its higher radiation tolerance than conventional materials like Si and GaAs.[1–3] Electronics used in satellites at low earth orbits (up to 1000 km) from the surface or solar expeditions are prone to continuous radiation exposure in the form of cosmic rays and ions of varied energies (from a few keV to hundreds of MeV) at relatively lower fluxes.[4] GaN-based devices can be simulated for better reliability and radiation hardness using swift heavy ions (oxygen in the present study) generated from the particle accelerator.

The properties of GaN can be altered by ion irradiation depending upon the type of radiation, energy, dose (fluence), doping concentration, etc.[5,6] For keV energies, the damage mechanism in GaN is reported to be controlled mainly by the generation of point defects and their migration, annihilation, and some other factors.[7–9] It is understood that the saturation level of lattice damage under ion irradiation is much lower for heavier ions than lighter ones.[10] The ions having energy higher than >4 MeV/u are known as swift heavy ions (SHIs). For such energies, electronic energy loss ($S_e$) plays a major role due to a larger magnitude than nuclear energy loss ($S_n$). For example, the $S_e/S_n$ ratio equals 1766 for 100 MeV O ions in GaN as calculated using SRIM 2008.[11] For keV energies, ions are implanted in the near-surface or depletion layer of the metal-semiconductor (*M-S*) junction, but for the SHI regime, ions penetrate through the GaN epitaxial layer (a few microns thick) up to the substrate. Therefore, controlled modification of the *M-S* interface can be done via defect creation or annealing existing defects without introducing external impurity atoms.[12]

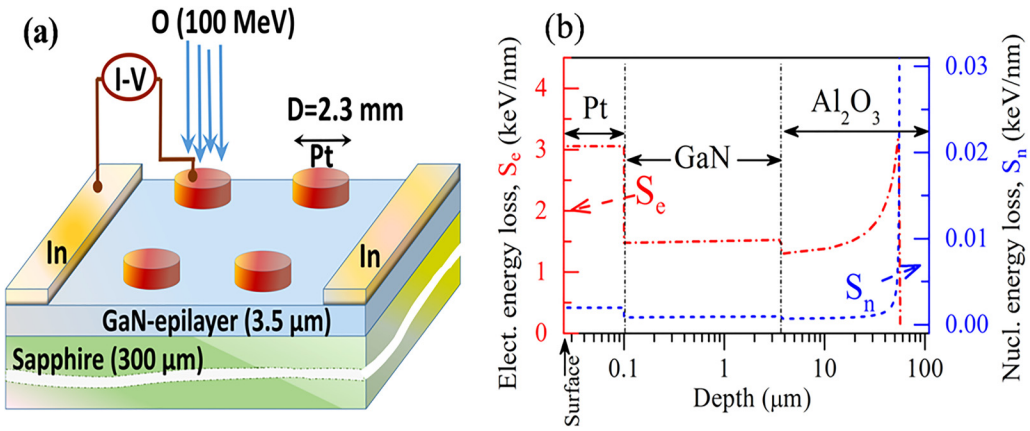


**FIG. 1.** (a) Schematic diagram of the irradiation experiment of the Pt/n-GaN Schottky barrier diode using O (100 MeV) ions, (b) variation of $S_e$ and $S_n$ vs ion's path length in Pt/GaN/sapphire (100 nm/3.6 $\mu$m/500 $\mu$m) target, simulated using SRIM/TRIM code.

Our previous investigation on 200 MeV Ag ion irradiation on Ni/GaN Schottky diodes showed that charge capture by defects created using SHI irradiation modified the electrical characteristics of the Schottky devices.[13,14] Similar studies by 50 MeV Ni ions on Au/GaN diodes found a decrease in Schottky barrier height (SBH) with increasing fluences.[15] Therefore, the basic understanding of transport phenomena in GaN Schottky diodes under SHI irradiation is not conclusive due to a limited number of experiments.

The *in situ* experimental investigations for GaN, particularly on the metal-semiconductor (*M-S*) interface, are not much explored. The present study reports the impact of 100 MeV O ions irradiation on Pt/GaN Schottky barrier diode (SBD) and GaN/sapphire epitaxial layer using *in situ* electrical characterizations and *ex situ* structural and optical characterizations (XRD, XTEM, and UV–Vis spectroscopy), respectively. The Pt metal was used for fabricating SBD on *n*-GaN because of its high work function (5.65 eV). *In situ* current–voltage measurements were performed on the same device after each fluence to avoid the device-specific effects in outcome caused by device-to-device variation.

## EXPERIMENTAL

Metal-organic chemical vapor deposition (MOCVD) technique was employed to grow 3.6 $\mu$m thick epitaxial GaN/sapphire layers at 900 °C temperature. The carrier concentration in the un-intentionally doped GaN layer was $2.5 \times 10^{17}$/cm$^3$ (by Hall effect measurement), RMS roughness was below 1 nm for a scan area of $10 \times 10\,\mu m^2$, and the density of dislocations was about $5 \times 10^8$/cm$^2$. Small pieces of $10 \times 10$ mm$^2$ were cut from the same wafer and cleaned for 10 min each in trichloroethylene, acetone, and isopropyl alcohol. A pre-metallization dip in an aqueous solution of HCl (1:1 v/v) was given for 1 min. Then, samples were rinsed in de-ionized water, followed by $N_2$ blow drying. Circular dots of 2 mm diameter of Pt (100 nm thick) were deposited by metal-shadow masking with an e-beam evaporation system. In the second step, ohmic contacts of indium were deposited, as shown in the schematic diagram [Fig. 1(a)]. Devices and epitaxial layer samples (for other characterizations) were then transferred to an irradiation chamber ($10^{-6}$ Torr) for 100 MeV $^{16}O^{7+}$ irradiation.[16] The variation of energy losses ($S_e$ and $S_n$) simulated using SRIM-2008[11] for 100 MeV O ion beams in the device structures is displayed in Fig. 1(b). SRIM calculations give values: $S_e = 1.476$ keV/nm, $S_n = 8.358 \times 10^{-4}$ keV/nm, $S_e/S_n = 1766$, and vacancies/ion = 9.5. For *in situ* investigations, Pt/GaN diodes were exposed to cumulative fluences and electrical characterizations were carried out after each fluence. A semiconductor analyzer (Agilent, B1500A) equipped with low-noise cables extended from the irradiation chamber using feedthrough was employed for *in situ* electrical measurements. To prevent channeling effects, a roughly 7° tilt angle was set between the sample surface normal and beam direction. Beam flux was kept constant at $6.25 \times 10^9$ ions/s/cm$^2$ for all samples. A Phillips pro-x-ray diffractometer was used for the characterization of structural modifications. Cross-sectional transmission electron microscopy (XTEM) for microstructural investigation of selected samples was recorded using an FEI Titan (80-300 STEM) system.

## RESULTS AND DISCUSSION

When Pt metal makes a junction with an *n*-GaN semiconductor, electrons flow from the semiconductor to the metal side to align the Fermi levels of both at the same level. Due to this, a barrier height is generated at the interface. In the absence of interface states, the barrier height ($\phi_0$) of the Schottky diode is given by the Schottky–Mott relation[17] as $\phi_0 = (\phi_m - \chi_S)$, where $\phi_m$ is the metal work function, and $\chi_S$ is the GaN electron affinity. $\phi_m = 5.61$ eV, and $\chi_S = 4.1$ eV for the Pt/GaN Schottky diode. For Schottky devices, the thermionic emission current transport process dominates, and the current–voltage relationship is given as[17,18]

$$I = I_O \exp\left(\frac{q[V - IR_S]}{nkT}\right), \quad (1)$$

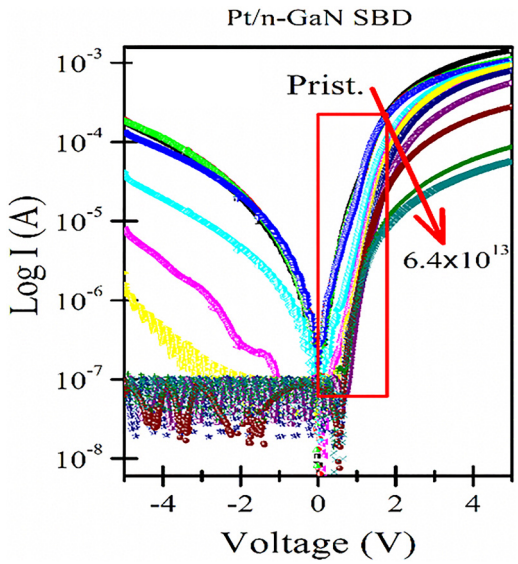


**FIG. 2.** Forward ln *I* vs *V* plot from *in situ* *I*–*V* measurements of irradiated diodes at different fluences; the linear portion for forward current shows inside the red box.

$$I_O = AA^{**}T^2 \exp\left(\frac{-q[\phi_b - \Delta\phi_b]}{kT}\right). \quad (2)$$

Here, $R_S$ is the series resistance that dominates at high voltages, i.e., in the saturation region of Schottky diode's forward I–V characteristics; $I_O$, $n$, $k$, and $A$ are reverse saturation current, ideality factor, Boltzmann's constant, and effective contact area of the diode, respectively. The Richardson constant is denoted by $A^{**}$ (26.4 A cm$^{-2}$ K$^{-2}$ for GaN), barrier height by $\phi_b$, and image force-induced barrier lowering by $\Delta\phi_b$. The current–voltage graph of Pt/GaN diodes (both pristine and irradiated) is displayed in Fig. 2. The slope and intercept of the linearly fitted forward ln *I*–*V* curve give the values of $n$ and $I_O$, respectively.[19,20] *SBH* was calculated from Eq. (2), while $R_S$ was determined using the Cheung and Cheung method.[21]

Figure 3 displays the changes in the diodes' $R_S$, $n$, and SBH characteristics as a function of the fluence. As visible from Fig. 3, SBH initially shows a negligible rise till a fluence of $7 \times 10^{11}$ ions/cm$^3$, but after this, there is a significant increase in its value. Commonly, improvement in SBH is associated with an improved interface. But here, the ideality factor also increases consistently with fluence, which means degradation of the device with increasing fluence. These contrasting variations in SBH and ideality factor (n) might only be understood qualitatively by considering Schottky barrier lowering ($\Delta\phi_b$) of ideal barrier height ($\phi_b$) as given by $\phi_{ap} = \phi_b - \Delta\phi_b$. As we know, $\Delta\phi_b \propto (N_D^+)^{1/4}$.[17] Here, $N_D^+$(dopant concentration) decreased with fluence because of possible charge carrier capture by SHI-induced defects at higher fluence values.[22] Hence, the lowering of $\Delta\phi_b$ factor causes an increase in the SBH. The drop in carrier concentration also resulted in a rise in series resistance with fluences evident from Fig. 3. Also, these

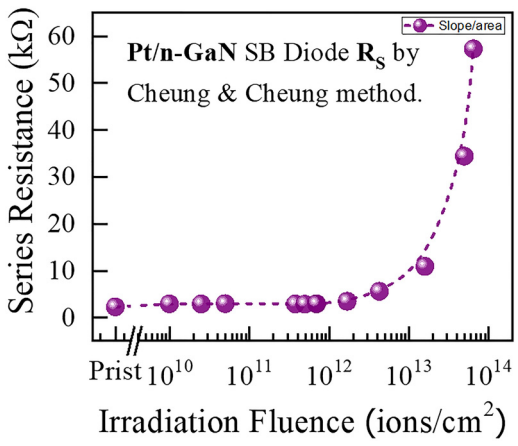


**FIG. 3.** Variation of series resistance ($R_s$) with fluence for the diodes. $R_S$ was determined using the Cheung and Cheung method.[21]

defect or trap levels might induce other current transport mechanisms like field emission, tunneling, leakage current at the contact periphery, and recombination current in the space-charge region in addition to a pure thermionic process.[23] This results in deviation in ideality factor values that are calculated by thermionic emission model. Similar results with other ions and energies have also been reported earlier[13,14,23,24] (Table I).

For detailed investigations on the effect of irradiation, offline measurements on irradiated epitaxial layers were also carried out. After irradiation, XRD and UV–Vis were performed, and the results are displayed in Fig. 4.

Figure 4(a) shows the XRD pattern for the pristine and irradiated GaN/sapphire epitaxial layer. The diffraction peaks indexed as (002) and (004) planes at 2θ = 34.60 and 72.93, respectively, correspond to the hexagonal wurtzite structure of GaN. Furthermore, the peaks corresponding to the sapphire substrate can also be seen in XRD. It is evident from the figure that the crystallinity of GaN epitaxial layers was maintained even after irradiation with oxygen

**TABLE I.** Various *in situ* parameters were measured from the electrical characteristics of irradiated Pt/GaN Schottky barrier diodes at various fluences.

| Fluence (ions/cm$^2$) | SBH (eV) | Ideality factor ($n$) | Series resistance (Ω) |
|---|---|---|---|
| Nil | 0.78 | 1.34 | 2 265.35 |
| $1.0 \times 10^{10}$ | 0.78 | 1.35 | 2 914.01 |
| $4.4 \times 10^{10}$ | 0.79 | 1.39 | 2 959.25 |
| $3.8 \times 10^{11}$ | 0.80 | 1.49 | 2 882.92 |
| $5.0 \times 10^{11}$ | 0.92 | 1.61 | 2 849.00 |
| $1.7 \times 10^{12}$ | 1.27 | 1.90 | 3 455.14 |
| $4.3 \times 10^{12}$ | 1.31 | 2.12 | 5 574.37 |
| $1.6 \times 10^{13}$ | 1.36 | 2.45 | 10 911.96 |
| $5.0 \times 10^{13}$ | 1.42 | 3.08 | 34 381.59 |
| $6.4 \times 10^{13}$ | 1.45 | 3.54 | 57 241.86 |

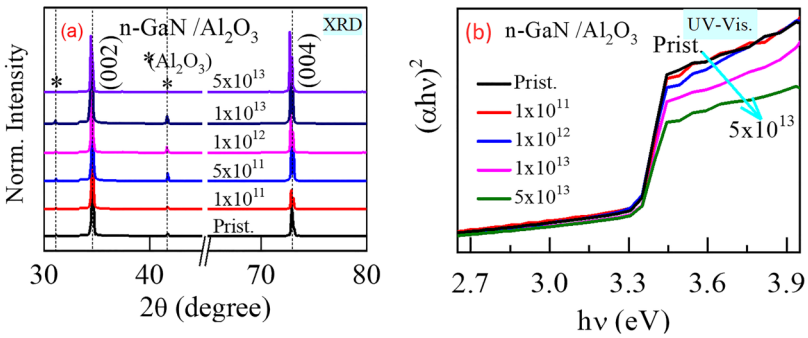


**FIG. 4.** Various *ex situ* measurements: (a) XRD and (b) UV–visible of pristine and irradiated GaN/sapphire epitaxial layers at various fluences.

ions. However, slight variation was observed in the (002) peak position representing the change in lattice parameter. The lattice parameter values show a negligible rise till a fluence of $5 \times 10^{11}$ ions/cm$^3$, but after this, there is a significant rise in its values, as can be observed from Table II. The ion beam induced modifications in the lattice parameters have also been observed by many researchers on GaN[25,26] and similar wide bandgap materials for ZnO thin films.[27] The passage of highly energetic ions results in the creation of point defects due to large electronic energy transfers. This creates a large amount of stress inside the system, which is responsible for the systematic shift in peak. The regular arrangement of atoms within the crystal lattice is disrupted when a GaN film is subjected to external stress caused by ion irradiation. This can result in the formation of point defects, which are localized irregularities in the crystal structure. The crystal lattice is strained by the presence of these point defects. This stress is the result of newly formed defects. As a result, neighboring atoms are subjected to forces that can cause them to move and adapt to accommodate the defects. This atomic rearrangement produces internal tension in the material. This interaction between stress and point defects can create a self-sustaining cycle due to a chain of displacement-replacement collision. The applied stress generates defects, and these defects can introduce additional stress, which, in turn, can generate further defects.[28]

To confirm the bandgap variation, UV–vis spectroscopy measurements were performed. After recording the optical absorption spectra of both pristine and irradiated GaN samples, Tauc's plot was used to calculate the bandgap [Fig. 4(b)]. The tangent of the line along the $x$ axis in Tauc's plot represents the bandgap. The slight variation in bandgap induced by the ion beam is given in Table II. Similar to the variation in XRD lattice parameters, there is a negligible variation for ion fluencies upto $5 \times 10^{11}$ ions/cm$^3$, but a noticeable change is observed for higher fluencies.

Furthermore, SHI irradiation induced band tailing effects, which are responsible for the modification in the optical properties of the semiconductors.[26,29] This is related to the irradiation induced traps in the deeper levels of energy bandgap. The change in bandgap is consistent with the changes observed in XRD patterns. Changes in the electronic structure can arise as a result of strain and defects, which introduce variations in the crystal lattice. Consequently, this has an impact on the bandgap. For example, alterations in lattice dimensions, such as expansion or contraction, can impact the energy levels associated with the valence and conduction bands, resulting in modifications to the bandgap.[30] We found in experimental data analysis that the lattice parameter increases with the increasing bandgap of the GaN epitaxial layer.

XTEM was used to analyze the microstructure of the GaN/sapphire epitaxial layer exposed to a fluence of $5.0 \times 10^{12}$ ions/cm$^2$ of 100 MeV $O^{7+}$ ions. The pictures obtained from this measurement are displayed in Fig. 5.

The XTEM images in Fig. 5 characterize the microstructural changes in the GaN/sapphire epitaxial layers shown by the zoomed

**TABLE II.** Various *ex situ* parameter measurements from XRD and UV–visible of pristine and irradiated GaN/sapphire epitaxial layers at various fluences.

| Samples | XRD Lattice parameter (Å) | UV–Vis Bandgap (eV) |
|---|---|---|
| Pristine | 5.176 | 3.325 |
| $1 \times 10^{11}$ | 5.178 | 3.325 |
| $5 \times 10^{11}$ | 5.179 | … |
| $1 \times 10^{12}$ | 5.187 | 3.326 |
| $1 \times 10^{13}$ | 5.191 | 3.329 |
| $5 \times 10^{13}$ | 5.193 | 3.335 |

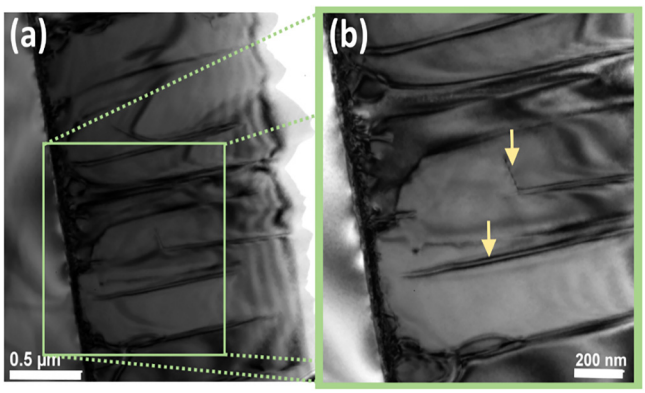


**FIG. 5.** (a) XTEM image of the 100 MeV $O^{7+}$ ions irradiated GaN/sapphire epitaxial layer at a fluence of $5 \times 10^{12}$ ions/cm$^2$, (b) zoomed view of part (a) marked for faults and dislocations.

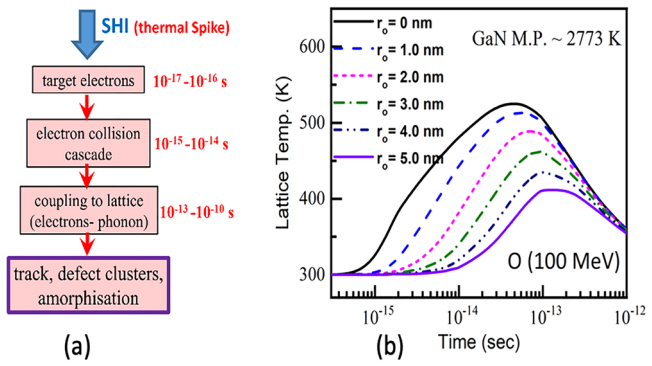


**FIG. 6.** (a) Schematic diagram showing the development of thermal spike in the lattice subsystem as a result of SHI irradiation, and (b) GaN's lattice temperature changes over time and at various radial separations from the path of 100 MeV O ions at room temperature. GaN has a melting temperature ($T_m$) of 2773 K.

view in Fig. 5(b). These images also show that the lattice mismatch at the interface of sapphire ($Al_2O_3$) and GaN caused stress, resulting in TEM contrasts at the interface. We observed the indication of microstructures and defects in the form of dislocations in the GaN epitaxial layers originating from the interface. Some dislocations can be seen in XTEM images as if they are transported from the top surface of the GaN layer. These are known as native dislocations. Most of the dislocations are aligned toward the growth direction [0001]. A TEM study also shows stacking faults/cracks-like structures marked by arrows in Fig. 5(b). However, no visible tracks or aligned defect clusters due to ion irradiations can be seen in the present study as observed in heavier Ag ion irradiation (200 MeV).[31]

The inelastic thermal spike model by Toulemonde *et al.*[32,33] can be used to analyze the defect creation caused by SHI irradiation. This model quantifies the creation of a track in the electronic energy loss domain for metals[33,34] and insulators[35,36] by connecting the initial transfer of energy from incoming ions to electrons with subsequent lattice damage. Electron–phonon coupling is responsible for regulating electron-to-lattice energy transfer. The mathematical framework is based on two concurrent differential equations given below, which relate to the duration and spread of the heat transports in the electronic subsystem and lattice subsystem,[32,33]

$$C_e(T_e)\frac{\partial T_e}{\partial t} = \frac{1}{r}\frac{\partial}{\partial r}\left[rK_e(T_e)\frac{\partial T_e}{\partial r}\right] - g(T_e - T_a) + A(r, t), \quad (3)$$

$$C_a(T_a)\frac{\partial T_a}{\partial t} = \frac{1}{r}\frac{\partial}{\partial r}\left[rK_a(T_a)\frac{\partial T_a}{\partial r}\right] - g(T_e - T_a). \quad (4)$$

Here, indexes $e$ and $a$ stand for electronic and lattice subsystems, respectively. The specific heat coefficient, temperature, and thermal conductivity are denoted by the symbols $C$, $T$, and $K$, respectively. The information about all the parameters vs $T$ is provided by the numerical solution of these equations. The electron–phonon mean free path is coupled to the electron–phonon coupling coefficient, denoted by the symbol $g$.[37] Table III lists all of the GaN parameter values along with the relevant references. The outcomes of thermal spike calculations (taking $\lambda$ as 5 nm) are shown in the schematic drawing [Fig. 6(a)]. The plot in Fig. 6(b) shows the variation of lattice temperature with time and space coordinates 40.8 (300 K).[37]

It can be seen that the highest lattice temperature for the O ion was substantially lower than the melting point for GaN (2773 K). The literature makes use of these nonlinear energy spike mechanisms for Si, and they are anticipated to likewise cause significant molecular effects in GaN.[41] The findings from *in situ* and *ex situ* measurements are consistent closely with the thermal spike model, which takes into account that local melting along the ions' path leads to a permanent phase transition. For oxygen ions, no such local melting and cluster/track formation takes place as local temperature could not rise beyond the melting temperature of GaN. This can be confirmed by TEM characterization, where no such large clusters of aligned or discontinuous defects/tracks are visible as a result of these phase transformations. However, small point defects and stress are produced due to ion energy losses as predicted by SRIM and confirmed by *in situ* electrical measurements. A single oxygen ion creates ~9.5 vacancies as calculated by SRIM/TRIM simulations.[31]

Similarly, other point defects, which are electrically active and might act as charge traps and scattering centres, are generated in ion irradiation. These point defects might not be structurally visible in TEM or XRD due to small sizes or lack of sufficient numbers to affect significant structural damage. For heavier ions like Ag or Au, the damage produced in the GaN layer per incident ion is greater and can be theoretically predicted and experimentally verified.[31]

## CONCLUSION

In summary, SHI irradiated Pt/n-GaN Schottky diodes were examined by *in situ I–V* measurement and GaN/sapphire epitaxial layer by *ex situ* structural (XTEM and XRD) and optical (UV–Vis) measurements. Based on these, it can be inferred that the ion beam induces point defects in the system due to the creation of large stress, which is responsible for the small variation in structural parameters and bandgap. However, the variation is not so significant that it could damage the crystal structure, thus indicating that ion energy and fluences used in the present study are insufficient to cause visible large structural changes or damages. The presence of small point defects and stress-related changes has been observed. *In*

**TABLE III.** Thermodynamical parameters of GaN used for thermal spike simulations.

| $\rho_S$ (g/cm$^3$) | $\rho_L$ (g/cm$^3$) | $T_m$ (K) | $T_V$ (K) | $Q_m$ (J/g) | $Q_V$ (J/g) | $\lambda$ (nm) | Therm. cond. (W cm$^{-1}$ °C$^{-1}$) | Specific heat (J g$^{-1}$ °C$^{-1}$) |
|---|---|---|---|---|---|---|---|---|
| 6.15[38] | 6.15[38] | 2773[39] | ~$10^4$ | 1599.05[38] | 8644.84[38] | 5.0[37] | 1.3 (300 K)[40] | 40.8 (300 K)[37] |

*situ I–V* electrical measurement of these diodes showed that SBH of the Pt/GaN Schottky diode increased with an increase in fluence of oxygen ion irradiation and was attributed to a decrease in carrier concentration. *I–V* measurements by fitting the thermionic emission current transport equation showed increments in ideality factor and series resistance with fluence. As calculated by the thermal spike model, the local temperature could not rise to the melting temperature of GaN to cause permanent large structural damages. However, the SRIM/TRIM showed that point defects were still generated, resulting in the trapping of charge carriers and, hence, modifications in the electrical properties of Pt/GaN Schottky diodes. Further experiments with similar and heavier ions can be carried out to provide a pinpoint conclusion. Hence, for a better understanding, more work is required in this direction.

## ACKNOWLEDGMENTS

A.K. acknowledges the IUAC New Delhi for providing the ion beam facility. We are thankful to Professor Rajendra Singh (IITD Delhi) for help in device fabrication. We are also thankful to Dr. Angelika Hähnel from Fraunhofer Institute for Microstructure of Materials and Systems IMWS, Germany, for carrying out XTEM measurements.

## AUTHOR DECLARATIONS

### Conflict of Interest

The authors have no conflicts to disclose.

### Author Contributions

**Kamal Singh:** Conceptualization (equal); Investigation (equal); Methodology (equal); Software (equal); Writing – original draft (equal). **Parmod Kumar:** Conceptualization (equal); Investigation (equal). **Vaishali Rathi:** Investigation (equal); Software (equal). **Tanuj Kumar:** Resources (supporting). **Ratnesh K. Pandey:** Conceptualization (supporting); Formal analysis (supporting). **D. Kanjilal:** Methodology (supporting); Supervision (equal); Visualization (equal). **Ranjeet K. Brajpuriya:** Supervision (equal); Visualization (equal). **Ashish Kumar:** Conceptualization (equal); Methodology (equal); Resources (equal); Supervision (equal); Writing – review & editing (equal).

## DATA AVAILABILITY

The data that support the findings of this study are available from the corresponding author upon reasonable request.

## REFERENCES

[1]P. J. Sellin, D. Hoxley, A. Lohstroh, A. Simon, W. Cunningham, M. Rahman, J. Vaitkus, and E. Gaubas, "Ion beam induced charge imaging of epitaxial GaN detectors," Nucl. Instrum. Methods. Phys. Res. A **531**, 82–86 (2004).
[2]A. Ionascut-Nedelcescu, C. Carlone, A. Houdayer, H. Von Bardeleben, J.-L. Cantin, and S. Raymond, "Radiation hardness of gallium nitride," IEEE Trans. Nucl. Sci. **49**, 2733–2738 (2002).
[3]J. Grant, R. Bates, W. Cunningham, A. Blue, J. Melone, F. McEwan, J. Vaitkus, E. Gaubas, and V. O'Shea, "GaN as a radiation hard particle detector," Nucl. Instrum. Methods. Phys. Res. A **576**, 60–65 (2007).
[4]R. Saxena, "Ground-level atmospheric neutron flux measurements in the 10–170 MeV range," Ph.D. dissertation (University of New Hampshire, 1990).
[5]S. O. Kucheyev, J. E. Bradby, J. S. Williams, C. Jagadish, M. V. Swain, and G. Li, "Deformation behavior of ion-beam-modified GaN," Appl. Phys. Lett. **78**, 156–158 (2001).
[6]S. O. Kucheyev, H. Timmers, J. Zou, J. S. Williams, C. Jagadish, and G. Li, "Lattice damage produced in GaN by swift heavy ions," J. Appl. Phys. **95**, 5360–5365 (2004).
[7]S. O. Kucheyev, J. S. Williams, and S. J. Pearton, "Ion implantation into GaN," Mater. Sci. Eng.: R: Rep. **33**, 51–108 (2001).
[8]S. O. Kucheyev, J. E. Bradby, C. P. Li, S. Ruffell, T. van Buuren, and T. E. Felter, "Effects of carbon on ion-implantation-induced disorder in GaN," Appl. Phys. Lett. **91**, 261905 (2007).
[9]P. A. Karaseov, A. Y. Azarov, A. I. Titov, and S. O. Kucheyev, "Density of displacement cascades for cluster ions: An algorithm of calculation and the influence on damage formation in ZnO and GaN," Semiconductors **43**, 691–700 (2009).
[10]S. O. Kucheyev, J. S. Williams, C. Jagadish, J. Zou, G. Li, and A. I. Titov, "Effect of ion species on the accumulation of ion-beam damage in GaN," Phys. Rev. B **64**, 035202 (2001).
[11]J. Ziegler, J. Biersack, and U. Littmark, "The stopping and range of ions in solids," in *Solids, The Stopping and Range of Ions in Matter*, edited by J. F. Ziegler (Pergamon, New York, 1985).
[12]S. O. Kucheyev, J. S. Williams, C. Jagadish, J. Zou, and G. Li, "Damage buildup in GaN under ion bombardment," Phys. Rev. B **62**, 7510–7522 (2000).
[13]A. Kumar, T. Kumar, A. Hähnel, D. Kanjilal, and R. Singh, "Dynamics of modification of Ni/n-GaN Schottky barrier diodes irradiated at low temperature by 200 MeV $Ag^{14+}$ions," Appl. Phys. Lett. **104**, 033507 (2014).
[14]A. Kumar, A. Hähnel, D. Kanjilal, and R. Singh, "Electrical and microstructural analyses of 200 MeV $Ag^{14+}$ion irradiated Ni/GaN Schottky barrier diode," Appl. Phys. Lett. **101**, 153508 (2012).
[15]V. Baranwal, S. Kumar, A. C. Pandey, and D. Kanjilal, "Effect of ion irradiation on current-voltage characteristics of Au/n-GaN Schottky diodes," J. Alloys Compd. **480**, 962–965 (2009).
[16]D. Kanjilal, S. Chopra, M. M. Narayanan, I. S. Iyer, V. Jha, R. Joshi, and S. K. Datta, "Testing and operation of the 15UD pelletron at NSC," Nucl. Instrum. Methods. Phys. Res. A **328**, 97–100 (1993).
[17]S. M. Sze and K. K. Ng, *Physics of Semiconductor Devices* (John Wiley & Sons, 2006).
[18]E. H. Rhoderick and R. H. Williams, *Metal-Semiconductor Contacts* (Clarendon, Oxford, 1988), pp. 1–70.
[19]A. Kumar, S. Vinayak, and R. Singh, "Micro-structural and temperature dependent electrical characterization of Ni/GaN Schottky barrier diodes," Curr. Appl. Phys. **13**, 1137–1142 (2013).
[20]A. Kumar, M. Kumar, R. Kaur, A. G. Joshi, S. Vinayak, and R. Singh, "Barrier height enhancement of Ni/GaN Schottky diode using Ru based passivation scheme," Appl. Phys. Lett. **104**, 133510 (2014).
[21]S. Cheung and N. Cheung, "Extraction of Schottky diode parameters from forward current-voltage characteristics," Appl. Phys. Lett. **49**, 85–87 (1986).
[22]A. Kumar, D. Kanjilal, V. Kumar, and R. Singh, "Defect formation in GaN epitaxial layers due to swift heavy ion irradiation," Radiat. Eff. Defects Solids **166**, 739–742 (2011).
[23]A. Kumar, J. Dhillon, S. Verma, P. Kumar, K. Asokan, and D. Kanjilal, "Identification of swift heavy ion induced defects in Pt/n-GaN Schottky diodes by *in-situ* deep level transient spectroscopy," Semicond. Sci. Technol. **33**, 085008 (2018).
[24]S. Kumar, V. K. Mariswamy, A. Kumar, A. Kandasami, and K. Sannathammegowda, "Enhancement of electrical parameters of Ni/n-GaN SBDs under remote and not in-flux gamma irradiation," ECS J. Solid State Sci. Technol. **9**, 093017 (2020).
[25]S. M. Basha, K. Asokan, P. Sangeetha, V. Ramakrishnan, and J. Kumar, "Micro Raman analysis of MOCVD grown gallium nitride epilayers irradiated with light and heavy ions," Mater. Chem. Phys. **132**, 494–499 (2012).

[26]V. S. Kumar, J. Kumar, P. Puviarasu, S. M. Basha, D. Kanjilal, and K. Asokan, "Effect of 100 MeV $Ni^{9+}$ion irradiation on MOCVD grown n-GaN," Phys. B **406**, 4210–4213 (2011).
[27]P. Kumar, H. K. Malik, S. Gautam, K. H. Chae, K. Asokan, and D. Kanjilal, "Modifications in room temperature ferromagnetism by dense electronic excitations in $Zn_{0.9}Mg_{0.1}O$ thin films," J. Alloys Compd. **710**, 831–835 (2017).
[28]M. Nastasi and J. W. Mayer, *Ion Implantation and Synthesis of Materials* (Springer Berlin Heidelberg, Berlin, 2006).
[29]E. Varadarajan, R. Dhanasekaran, D. K. Avasthi, and J. Kumar, "Structural, optical and electrical properties of high energy irradiated Cl-VPE grown gallium nitride," Mater. Sci. Eng. B **129**, 121–125 (2006).
[30]C. Zhu *et al.*, "Strain engineering in perovskite solar cells and its impacts on carrier dynamics," Nat. Commun. **10**(1), 815 (2019).
[31]A. Kumar, R. Singh, P. Kumar, U. B. Singh, K. Asokan, P. A. Karaseov, A. I. Titov, and D. Kanjilal, "*In-situ* transport and microstructural evolution in GaN Schottky diodes and epilayers exposed to swift heavy ion irradiation," J. Appl. Phys. **123**, 161539 (2018).
[32]M. Toulemonde, C. Dufour, and E. Paumier, "Transient thermal process after a high-energy heavy-ion irradiation of amorphous metals and semiconductors," Phys. Rev. B **46**, 14362–14369 (1992).
[33]C. Dufour, A. Audouard, F. Beuneu, J. Dural, J. P. Girard, A. Hairie, M. Levalois, E. Paumier, and M. Toulemonde, "A high-resistivity phase induced by swift heavy-ion irradiation of Bi: A probe for thermal spike damage?," J. Phys.: Condens. Matter **5**, 4573 (1993).
[34]Z. G. Wang, C. Dufour, E. Paumier, and M. Toulemonde, "The $S_e$ sensitivity of metals under swift-heavy-ion irradiation: A transient thermal process," J. Phys.: Condens. Matter **6**, 6733 (1994).
[35]A. Meftah, J. M. Costantini, N. Khalfaoui, S. Boudjadar, J. P. Stoquert, F. Studer, and M. Toulemonde, "Experimental determination of track cross-section in $Gd_3Ga_5O_{12}$ and comparison to the inelastic thermal spike model applied to several materials," Nucl. Instrum. Methods Phys. Res. B **237**, 563–574 (2005).
[36]A. Meftah, F. Brisard, J. M. Costantini, E. Dooryhee, M. Hage-Ali, M. Hervieu, J. P. Stoquert, F. Studer, and M. Toulemonde, "Track formation in $SiO_2$ quartz and the thermal-spike mechanism," Phys. Rev. B **49**, 12457–12463 (1994).
[37]D. J. Suntrup, G. Gupta, H. Li, S. Keller, and U. K. Mishra, "Measurement of the hot electron mean free path and the momentum relaxation rate in GaN," Appl. Phys. Lett. **105**, 263506 (2014).
[38]O. Madelung, U. Rössler, and M. Schulz, "Gallium nitride (GaN), thermodynamical parameters, vaporization," in *Group IV Elements, IV-IV and III-V Compounds. Part b—Electronic, Transport, Optical and Other Properties* (Springer Berlin Heidelberg, 2002).
[39]S. Porowski, "Growth and properties of single crystalline GaN substrates and homoepitaxial layers," Mater. Sci. Eng. B **44**, 407–413 (1997).
[40]E. Sichel and J. Pankove, "Thermal conductivity of GaN, 25–360 K," J. Phys. Chem. Solids **38**, 330 (1977).
[41]S. O. Kucheyev, J. S. Williams, A. I. Titov, G. Li, and C. Jagadish, "Effect of the density of collision cascades on implantation damage in GaN," Appl. Phys. Lett. **78**, 2694 (2001).